HETEROCYCLES, Vol. 102, No. 12, 2021, pp. -. © 2021 The Japan Institute of Heterocyclic Chemistry
Received, 18th August, 2021, Accepted, 10th September, 2021, Published online, 14th September, 2021
DOI: 10.3987/COM-21-14538

OSCILLATOXIN E AND ITS C7 EPIMER SHOW DISTINCT GROWTH INHIBITION PROFILES AGAINST SEVERAL CANCER CELL LINES

Yusuke Hanaki,[1]* Yusuke Araki,[2] Toshio Nishikawa,[2] and Ryo C. Yanagita[1]

[1]Faculty of Agriculture, Kagawa University, Kagawa 761-0795, Japan. E-mail: hanaki.yusuke@kagawa-u.ac.jp. [2]Graduate School of Bioagricultural Sciences, Nagoya University, Nagoya 464-8601, Japan.

Abstract – Oscillatoxins (OTXs) are naturally occurring polyketides produced by some marine cyanobacteria. We have recently reported the total synthesis and *in vitro* biological activities of OTX-D, E, and F. Their spiro-ether structure was synthesized with an intramolecular Mukaiyama aldol reaction as a key step. Although the desired isomer was stereoselectively obtained, some amount of its C7 epimer was also produced as a byproduct. Using the C7 epimer, we investigated the effect of stereochemistry at the spiro-center of OTX-E (**1**) on its antiproliferative activity against several cancer cell lines. Growth inhibitory activity of **1** and its C7 epimer **2** was not strong, but they showed different efficacy profiles from each other. This result suggests that our synthetic method for OTXs would contribute to not only total synthesis of natural products but also to construction of chemical libraries containing unique biologically active compounds.

Oscillatoxins (OTXs) and aplysiatoxins (ATXs) are polyketide-type natural products isolated from some cyanobacteria species and the digestive gland of sea hare *Stylocheilus longicauda* that feeds on them (Figure 1).[1] Several tens of derivatives with diverse carbon skeletons have been isolated so far,[2-9] and they are thought to be biosynthesized from a common intermediate.[4] Their structural diversity seems to be related to their diverse biological functions. Macrolide-type analogs such as OTX-A, ATX, and neo-ATX-A activate protein kinase C (PKC) and show potent tumor-promoting and proinflammatory activities.[10,11] Since PKC, a family of serine/threonine kinases, plays important roles in cellular signal transduction, simplified ATX analogs have been developed as potential medicinal seed compounds to treat intractable diseases such as cancer, AIDS, and Alzheimer's disease.[12-14] OTX-D was also reported to show anti-leukemic activity against the L1210 cell line, though the experimental details have not been described.[15] Although Toshima *et al.* achieved the first total synthesis of OTX-D and 30-methyl-OTX-D,[15] they did not

validate their biological activity. Recently, some derivatives including OTX-D, OTX-E (**1**), and neo-debromo-ATX-B were revealed to inhibit potassium channel Kv1.5,[5] but the relevance to their cytotoxicity was not described. In addition, toxicity of OTXs to cancer cells, brine shrimps, and marine diatoms have been investigated by several groups,[3-9] but their mode of actions have not been revealed.

Considering the unique chemical structures and biological activities of OTXs, collecting these derivatives from cyanobacteria would expand the chemical space for drug discovery. However, the site and time where cyanobacteria occur are limited and unpredictable. Moreover, the amount of each isolated OTX derivative was only several milligrams. Therefore, developing a reliable synthetic method is desired as a way to address the problem of supply. Inspired by a proposed biosynthetic pathway of OTXs, Nishikawa's group initiated a study on the collective synthesis of these natural products from a common intermediate.[16] As part of this research, total synthesis and biological evaluation of OTX-D, 30-methyl-OTX-D, OTX-E (**1**), and OTX-F, have recently been reported.[17] Cytotoxic potency of these derivatives toward leukemia and cancer cell lines were similar, except that OTX-F showed a slightly stronger anti-proliferative activity against a few cell lines. This result suggested that functional groups linked via ester linkage at position 1 do not have significant effects on their cytotoxicity, and various tags can be introduced there without affecting their cytotoxic activities.

Based on the above results, the spiro-ether, attached side chain, or both should be essential for the cytotoxicity of OTXs. Specifically, the spiro-ether core is a hallmark structure of some OTX derivatives. In ATX/OTX-A and their analogs, modification of the spiro-acetal structure and functional groups on the moiety significantly influence their anti-proliferative activity and PKC isozyme-selectivity.[18-21] Hence, we planned the synthesis of the C7 epimer of **1** (7-*epi*-OTX-E, **2**) to reveal the contribution of OTXs' spiro-ether structure to their cytotoxicity. Because we have already obtained **2'** as an undesired isomer during the total synthesis of OTX-D, E, and F (Scheme 1),[16,17] **2** would be readily provided by deprotection of the TIPS group of **2'**. Our recent study showed that the cytotoxic potency of OTXs partly depends on their molecular hydrophobicity,[22] since the hydrophobic derivatives would be trapped by serum components such as albumin. On the other hand, we expected that the difference in cytotoxicity of **1** and **2** would precisely reflect the difference in their affinity for an unknown molecular target responsible for their biological activities because their hydrophobicity is similar to each other. Moreover, various structures can be concisely introduced to **1** and **2** by trans-esterification of the β-keto-ester, enabling them to provide molecular probes to identify target proteins of OTXs in the future. Thus, in this study, we compared the antiproliferative activity of **2** with that of **1** to discuss the role of the spiro-structure in OTXs' biological activities.

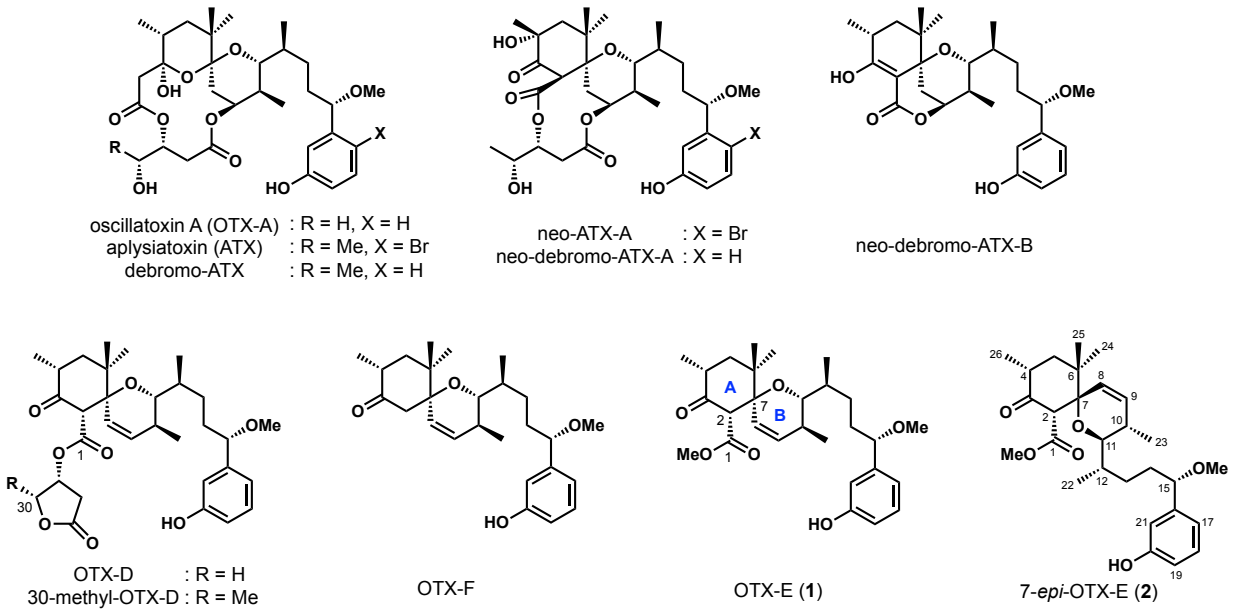

Figure 1. Structure of oscillatoxins and aplysiatoxins

In our previous synthetic study on OTX-D, E, and F, we found that treating the intermediate **A** with $BF_3 \cdot OEt_2$ afforded a mixture of three diastereomers **1'**, **2'**, and **3'** in 59%, 25%, and 6% yield, respectively (Scheme 1).[16,17] Since the production ratio of these diastereomers was thermodynamically determined, the production of some amount of undesired diastereomers was inevitable. Our previous NMR analysis suggested that the A-ring of **2'** is a chair conformation similar to that of **1'**, while that of **3'** is an equilibrium mixture of the chair and twist-boat conformations.[16] In addition, **3'** would be easily converted to thermodynamically favored **2'** under basic or acidic conditions. Therefore, we utilized **2'** to evaluate the effect of stereochemistry at the spiro-center on the growth inhibitory activity. Compound **2** was synthesized by deprotection of the TIPS group of **2'** with TBAF in the presence of AcOH.

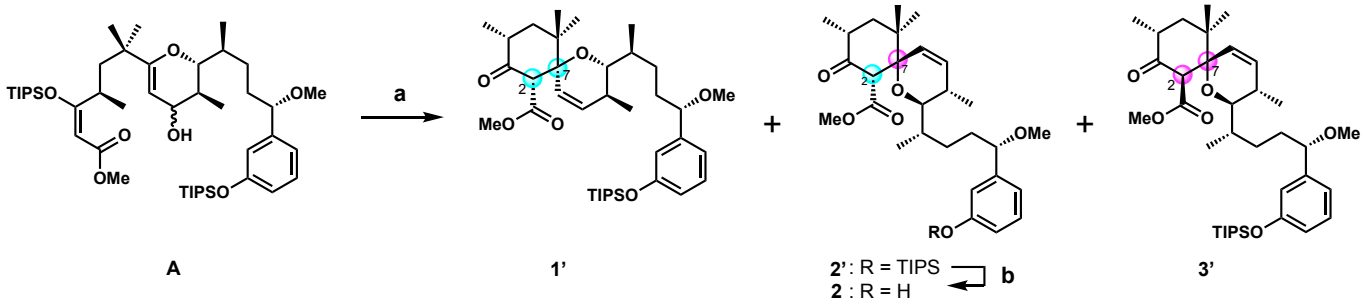

Scheme 1. Synthesis of 7-*epi*-OTX-E (**2**). (a) $BF_3 \cdot OEt_2$, MS4A, CH_2Cl_2, **1'**: 59%, **2'**: 25%, **3'**: 6%. (b) TBAF, AcOH, THF, 90%.

First, we examined the cytotoxicity of **2** toward the HHUA endometrial cancer cell line because our previous study showed that OTXs potently inhibited the growth of HHUA cells.[22] As shown in Figure 2, **2** showed about three times weaker cytotoxicity than **1**. The IC_{50} values of **1** and **2** (and the 95% confidence

interval) were 3.2 (2.9–3.6) and 9.2 (7.0–12.2) μM, respectively. Accordingly, the stereochemistry at position 7 is important to inhibit the growth of HHUA cells. Although **1** was reported to show potent blocking activity against potassium channel Kv1.5,[5] our previous result suggested that Kv1.5 was not involved in its cytotoxicity; OTX-F, a weak Kv1.5 blocker, also showed comparable cytotoxicity in HHUA cells.[22] There should be an unknown target which **1** interacts with better than **2**.

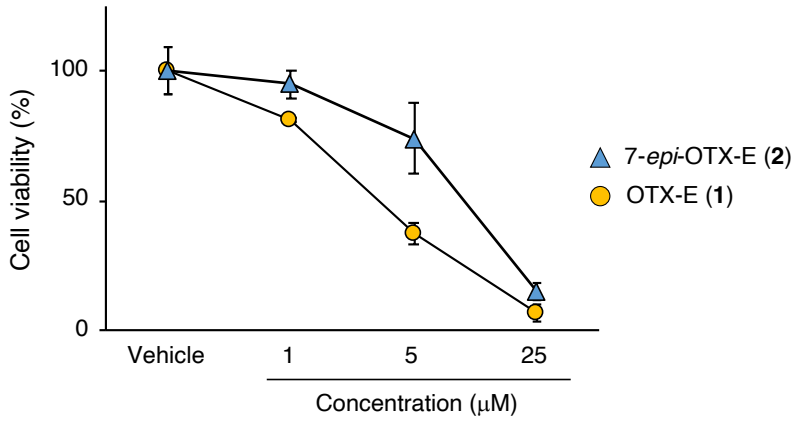

Figure 2. Cytotoxicity of **1** and **2** in HHUA cells. HHUA cells were treated with indicated concentrations of **1** or **2** for 48 h. Thereafter, cell number was determined using a MTT assay. Cell viability is plotted as a percentage relative to the vehicle group. The average and standard deviation are presented (n = 3).

We further examined the antiproliferative activity of **2** using a panel of 39 human cancer cell lines established by Yamori and colleagues.[23] The efficacy profile is useful for predicting the mode of action of natural products since compounds that have the same growth-inhibitory mechanism would show similar cell line selectivity. The database of standard compounds, including anticancer agents and inhibitors of cellular signal transduction, is available as a reference. The profiles of **1** and **2** are shown in Figure 3, and the GI_{50} value (the concentration required to inhibit cell growth by 50%) measured against each cell line is listed in Supporting Information. The mean-graph midpoints (MG-MID, average of log GI_{50} for each cell line) of **1** and **2** were quite similar, but there were some differences in their cell line selectivity. While **1** showed relatively stronger cytotoxicity toward MKN74 and MKN-B stomach cell lines (1.6 and 1.5 times the average for 39 cell lines), **2** did not have a marked preference for them. The inversion of stereochemistry at the spiro-center attenuated the cytotoxicity to these cell lines, similar to the case of HHUA. On the other hand, **2** exhibited a modest selectivity to some other cell lines such as DMS114 and BSY-1 (1.5 and 1.2 times the average for 39 cell lines). DMS114 is relatively sensitive to not only **2** but also **1** and other OTXs,[17] suggesting that their common structures, including a B-ring and the side chain, could be important for growth inhibition against this cell line. On the contrary, **1** did not show a preference for the BSY-1 cell line, unlike **2**. Overall, the Pearson's correlation coefficient between log GI_{50} fingerprints of **1** and **2** was relatively low (r = 0.55).[24] Their profiles are also not correlated to those of other standard compounds and

debromo-ATX, a potent PKC activator. These results suggest that **1** and **2** may have novel and distinct antiproliferative mechanisms.

We performed molecular modeling to demonstrate the difference between **1** and **2** in three-dimensional structure. Their side-chains at position 11 were replaced to an isopropyl group to simplify the calculation. As shown in Figure 4, the stereoinversion at the spiro-center alters the spatial arrangement of functional groups and heteroatoms on the spiro-ether moiety. Therefore, **1** and **2** may occupy different portions of chemical apace and interact with distinct target molecules.

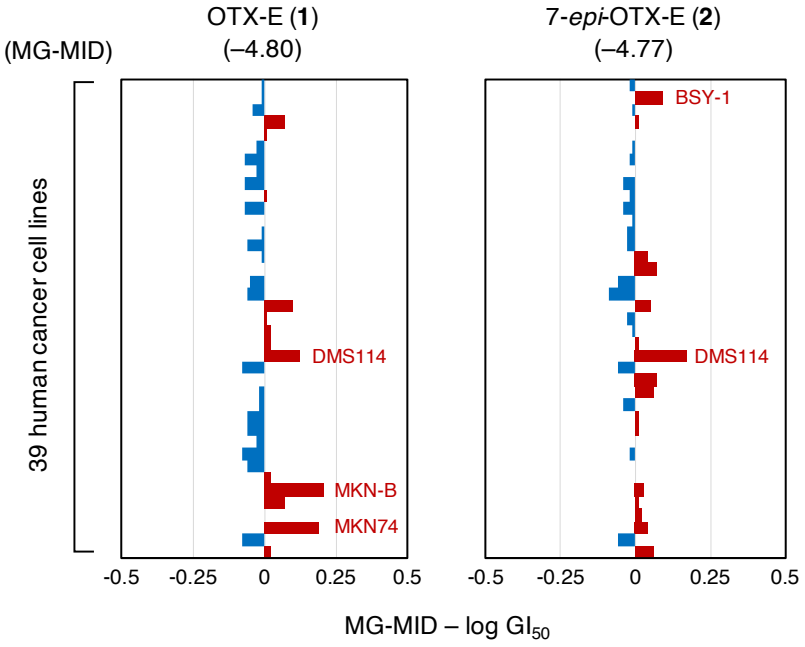

Figure 3. Fingerprints against human cancer cell lines. Difference between log GI_{50} for each cell line and MG-MID (mean-graph midpoint). Data for the following 39 cell lines are listed in top-to-bottom order: breast (HBC-4, BSY-1, HBC-5, MCF-7, MDA-MB-231); CNS (U251, SF-268, SF-295, SF-539, SNB-75, SNB-78); colon (HCC2998, KM-12, HT-29, HCT-15, HCT-116); lung (NCI-H23, NCI-H226, NCI-H522, NCI-460, A549, DMS273, DMS 114); melanoma (LOX-IMVI); ovarian (OVCAR-3, OVCAR-4, OVCAR-5, OVCAR-8, SK-OV-3); renal (RXF-631L, ACHN); stomach (St-4, MKN1, MKN-B, MKN-A, MKN45, MKN74); and prostate (DU-145, PC-3). Data for **1** was cited from our previous report.[17]

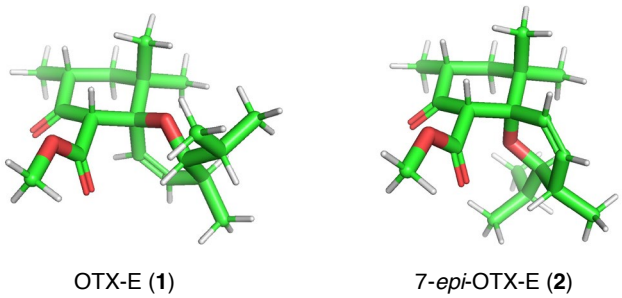

Figure 4. Three-dimensional structure of spiro-ether core of **1** and **2**

In this study, we synthesized the C7 epimer of **1** (**2**) and compared its antiproliferative activity with that of **1**. Interestingly, their efficacy profiles were partly different from each other. However, the observed difference in the GI_{50} values was small, probably due to the fact that the basic cytotoxicities of **1** and **2** were not strong. The next step should be to develop more potent analogs and precisely determine which structural factors of OTXs contribute to the selectivity of each cell line. Such analogs will also be useful for providing molecular probes to identify the target proteins responsible for the unique antiproliferative activity of OTXs. Moreover, it is remarkable that we efficiently obtained a set of unique compounds that showed distinct cell line selectivity in short steps from a common intermediate. Recently, chemical libraries containing sp^3-rich natural products and their analogs have been highly valued in medicinal chemistry.[25] Traditional chemical libraries contain a large number of compounds but show planar and aromatic characteristics because they have been constructed using easy reactions like sp^2-sp^2 cross-coupling.[26] These numerous but localized compounds cannot fully occupy druggable chemical space, resulting in a low hit rate. On the other hand, OTX is a family of sp^3-rich natural products and exhibited different efficacy profiles depending on a small structural modification. Therefore, OTXs and related analogs might have multiple and unique cytotoxic mechanisms and enable access to a wider chemical space. We have already achieved total synthesis of some OTXs from a common intermediate,[16,17] and synthetic study toward the collective synthesis of newly isolated derivatives is currently in progress. Further studies on the chemistry and biology of OTXs using our synthetic method could help increase the diversity and quality of chemical libraries in the future.

EXPERIMENTAL

General remarks

Optical rotations were measured with a P-1010 digital polarimeter (JASCO, Tokyo, Japan). ^{1}H and ^{13}C NMR were recorded on a JNM-ECZ500R (JEOL, Tokyo, Japan). Chemical shifts are reported in ppm relative to the residual solvent (^{1}H NMR: $CDCl_3$ as $\delta = 7.26$, ^{13}C NMR: $CDCl_3$ as $\delta = 77.2$). High-resolution electrospray ionization mass spectra (HR-ESI-qTOF-MS) were recorded on a micrOTOF II (Bruker Daltonics, Billerica, MA, USA). Wakogel® C-300 (silica gel, FUJIFILM Wako Pure Chemical Corporation, Osaka, Japan) was used for column chromatography. All other chemicals and regents were purchased from chemical companies and used without further purification.

Synthesis of 2

Compound 2'. Compound **2'** was synthesized as reported previously.[17] **^{1}H NMR**: (500 MHz, $CDCl_3$, 0.036 M): δ 0.81 (3H, d, J = 7.4 Hz), 0.87 (3H, d, J = 6.9 Hz), 0.90 (3H, s), 0.98 (3H, d, J = 6.3 Hz), 1.09 (18H, d, J = 7.5 Hz), 1.21 (3H, s), 1.23-1.34 (5H, m), 1.47 (1H, dd, J = 13.2, 6.3 Hz), 1.55-1.65 (2H, m), 1.74 (1H, t, J = 13.5 Hz), 1.81 (1H, m), 2.27 (1H, m), 2.41 (1H, m), 3.17 (3H, s), 3.20 (1H, d, J = 9.7 Hz), 3.60 (3H, s), 3.72 (1H, s), 3.98 (1H, t, J = 6.6 Hz), 5.64 (1H, dd, J = 10.3, 2.8 Hz), 5.77 (1H, d, J = 10.3 Hz),

6.76-6.81 (3H, m), 7.15 (1H, t, J = 7.7 Hz) ppm; **^{13}C NMR**: (125 MHz, $CDCl_3$, 0.036 M): δ 12.8 (3C), 12.8, 14.5, 17.1, 18.1 (6C), 24.7, 26.7, 29.3, 30.8, 34.6, 36.5, 40.7, 41.2, 45.2, 51.2, 56.6, 62.7, 80.3, 83.5, 84.4, 118.2, 119.3, 120.0, 124.0, 129.2, 136.6, 144.0, 156.4, 168.0, 205.1 ppm; **HR-ESI-qTOF-MS**: *m/z* 651.4067 ($[M + Na]^+$). Calcd. for $C_{37}H_{60}O_6SiNa$ 651.4051; **[α]$_D$**: +67 (*c* 1.4, MeOH, 22.1 °C).

7-*epi*-Oscillatoxin E (2). To spiro-ether **2'** (26.5 mg, 42.2 μmol) was added the solution of TBAF (16.6 mg, 63.3 μmol) in AcOH (4.8 μL, 84.4 μmol) and THF (1.5 mL) at 4 °C. The mixture was allowed to warm to room temperature and stirred for 45 min. The mixture was diluted with H_2O (3 mL). The organic layer was separated and the aqueous layer was extracted with EtOAc (3 mL × 3). The combined organic layer was washed with brine, dried over Na_2SO_4, filtered, and concentrated under reduced pressure. The residue was purified by column chromatography (silica gel 2 g, EtOAc/hexane = 1/10 to 1/3) to afford 7-*epi*-OTX-E (**2**) (18.0 mg, 38.1 μmol, 90%) as a colorless oil. **^{1}H NMR**: (500 MHz, $CDCl_3$, 0.031 M): δ 0.81 (3H, d, J = 7.4 Hz, H_3-23), 0.86 (3H, d, J = 6.9 Hz, H_3-22), 0.89 (3H, s, H_3-24), 0.97 (3H, d, J = 6.3 Hz, H_3-26), 1.21 (3H, s, H_3-25), 1.23-1.33 (2H, m, H_2-13), 1.44 (1H, dd, J = 13.9, 6.6 Hz, H_{eq}-5), 1.55-1.64 (2H, m, H-12, H-14a), 1.68 (1H, t, J = 12.9 Hz, H_{ax}-5), 1.82 (1H, m, H-14b), 2.27 (1H, m, H-10), 2.41 (1H, m, H-4), 3.21 (3H, s, -OCH_3), 3.21 (1H, m, H-11), 3.60 (3H, s, -COOCH_3), 3.72 (1H, s, H-2), 4.02 (1H, t, J = 6.9 Hz, H-15), 5.64 (1H, dd, J = 10.3, 2.3 Hz, H-8), 5.77 (1H, d, J = 10.3 Hz, H-9), 6.72-6.81 (3H, m, H-17, H-19, H-21), 7.17 (1H, t, J = 7.8 Hz, H-18) ppm; **^{13}C NMR**: (125 MHz, $CDCl_3$, 0.031 M): δ 13.0, 14.5, 17.1, 24.7, 26.7, 29.3, 30.5, 34.8, 36.4, 40.7, 41.3, 45.2, 51.3, 56.7, 62.7, 80.2, 83.6, 84.4, 113.4, 114.7, 119.5, 123.9, 129.6, 136.6, 144.3, 156.1, 168.0, 205.4 ppm; **HR-ESI-qTOF-MS**: *m/z* 495.2697 ($[M + Na]^+$). Calcd. for $C_{28}H_{40}O_6Na$ 495.2717; **[α]$_D$**: +80 (*c* 0.31, MeOH, 21.6 °C).

Cell culture

The human endometrial cancer cell line, HHUA (RCB0658), was provided by RIKEN BRC through the National Bio-Resource Project of the MEXT/AMED (Tsukuba, Japan). The cells were cultured in Ham's F-12 medium with 10% heat-inactivated FBS, 1 mM L-glutamine, 100 IU/mL penicillin, and 100 μg/mL streptomycin in a 5% CO_2 humidified incubator maintained at 37 °C.

Cytotoxicity assay toward HHUA cell line

HHUA cells were seeded in 96-well plates at a density of 5,000 cells/well in 200 μL of medium and were allowed to adhere overnight. A test compound in 0.5 μL of DMSO was added to each well, and the cells were incubated for 48 h. A solution of MTT (100 μg) in PBS buffer (20 μL) was then added to each well, and the plate was incubated for an additional 4 h. The medium was removed by aspiration, the generated formazan was dissolved in 150 μL of DMSO, and the absorbance was measured at 570 nm using a Multiskan FC microplate reader (Thermo Fisher Scientific, Waltham, MA, USA). The cell viability (%) in the presence of each concentration of test compound was plotted as a percentage relative to the vehicle

group, and IC_{50} and 95% confidence interval were determined by nonlinear regression to complementary error function using the R software version 4.1.0.

Measurement of cell proliferation inhibition against 39 human cancer cell lines

We employed a panel of 39 human cancer cell lines established by Yamori and colleagues according to the NCI method with modification, and measured cell proliferation inhibition as reported previously.[23]

Molecular modeling study

Side-chains at position 11 of **1** and **2** were replaced with an isopropyl group to simplify the calculation. Initial geometric optimization was performed with the MMFF94 force field using the Avogadro (version 1.2.0) software.[27] Final geometric optimization and frequency analysis were conducted at the ωB97X-D/6-311+G(d,p) level of theory using the Gaussian 16 (Revision C.01) program package.[28]

ACKNOWLEDGEMENTS

We grateful to Ms. Tsugumi Shiokawa and Dr. Hiroko Tada (Okayama University) for MS measurements. The DFT calculation was performed using Research Center for Computational Sciences, Okazaki, Japan. We thank the Molecular Profiling Committee, Grant-in-Aid for Scientific Research on Innovative Areas "Advanced Animal Model Support (AdAMS)" from the Ministry of Education, Culture, Sports, Science and Technology, Japan (JSPS KAKENHI Grant Number JP 16H06276) for the support. This work was also supported by JSPS KAKENHI (grant number 21K14793 to Y.H. and 19H02896 to T.N.).

REFERENCES

1. Y. Kato and P. J. Scheuer, *J. Am. Chem. Soc.*, 1974, **96**, 2245.
2. M. Entzeroth, A. J. Blackman, J. S. Mynderse, and R. E. Moore, *J. Org. Chem*., 1985, **50**, 1255.
3. B. N. Han, T. T. Liang, L. J. Keen, T. T. Fan, X. D. Zhang, L. Xu, Q. Zhao, S. P. Wang, and H. W. Lin, *Org. Lett*., 2018, **20**, 578.
4. H. Nagai, M. Watanabe, S. Sato, M. Kawaguchi, Y. Y. Xiao, K. Hayashi, R. Watanabe, H. Uchida, and M. Satake, *Tetrahedron*, 2019, **75**, 2486.
5. Y. H. Tang, J. Wu, T. T. Fan, H. H. Zhang, X. X. Gong, Z. Y. Cao, J. Zhang, H. W, Lin, and B. N. Han, *RSC Adv.*, 2019, **9**, 7594.
6. H. H. Zhang, X. K. Zhang, R. R. Si, S. C. Shen, T. T. Liang, T. T. Fan, W. Chen, L. H. Xu, and B. N. Han, *Toxins*, 2020, **12**, 733.
7. Y. H. Tang, T. T. Liang, T. T. Fan, L. J. Keen, X. D. Zhang, L. Xu, Q. Zhao, R. Zeng, and B. N. Han, *Nat. Prod. Res*., 2020, **34**, 2151.
8. T. T. Fan, H. H. Zhang, Y. H. Tang, F. Z. Zhang, and B. N. Han, *Mar. Drugs*, 2019, **17**, 652.
9. K. Iguchi, M. Satake, Y. Nishio, B. T. Zhang, K. Kawashima, H. Uchida, and H. Nagai, *Heterocycles*, 2021, **102**, 1287.

10. J. P. Arcoleo and I. B. Weinstein, *Carcinogensis*, 1985, **6**, 213.
11. H. Fujiki and T. Sugimura, *Adv. Cancer Res*., 1987, **49**, 223.
12. Y. Nakagawa, R. C. Yanagita, N. Hamada, A. Murakami, H. Takahashi, N. Saito, H. Nagai, and K. Irie, *J. Am. Chem. Soc*., 2009, **131**, 7573.
13. K. Irie and R. C. Yanagita, *Chem. Rec.*, 2014, **14**, 251.
14. K. Irie, *Biosci. Biotechnol. Biochem*., 2020, **84**, 1.
15. H. Toshima, T. Goto, and A. Ichihara, *Tetrahedron Lett*., 1995, **36**, 3373.
16. Y. Nokura, Y. Araki, A. Nakazaki, and T. Nishikawa, *Org. Lett*., 2017, **19**, 5992.
17. Y. Araki, Y. Hanaki, M. Kita, K. Hayakawa, K. Irie, Y. Nokura, A. Nakazaki, and T. Nishikawa, *Biosci. Biotechnol. Biochem*., 2021, **85**, 1371.
18. M. Kikumori, R. C. Yanagita, H. Tokuda, N. Suzuki, H. Nagai, K. Suenaga, and K. Irie, *J. Med. Chem.*, 2012, **55**, 5614.
19. M. Kikumori, R. C. Yanagita, H. Tokuda, K. Suenaga, H. Nagai, and K. Irie, *Biosci. Biotechnol. Biochem.*, 2016, **80**, 221.
20. K. Hayakawa, Y. Hanaki, H. Tokuda, R. C. Yanagita, Y. Nakagawa, M. Okamura, S. Dan, and K. Irie, *Heterocycles*, 2018, **97**, 478.
21. Y. Ashida, R. C. Yanagita, Y. Kawanami, M. Okamura, S. Dan, and K. Irie, *Heterocycles*, 2019, **99**, 942.
22. Y. Hanaki, Y. Araki, T. Nishikawa, and R. C. Yanagita, *Fundam. Toxicol. Sci*., 2021, **8**, 69.
23. T. Yamori, A. Matsunaga, S. Sato, K. Yamazaki, A. Komi, K. Ishizu, I. Mita, H. Edatsugi, Y. Matsuba, K. Takezawa, O. Nakanishi, H. Kohno, Y. Nakajima, H. Komatsu, T. Andoh, and T. Tsuruo, *Cancer Res.*, 1999, **59**, 4042.
24. W. Z. Guo, Y. Wang, E. Umeda, I. Shiina, S. Dan, and T. Yamori, *Biol. Pharm. Bull.*, 2013, **36**, 1008.
25. B. J. Huffman, S. Chen, J. L. Schwarz, R. E. Plata, E. N. Chin, L. L. Lairson, K. N. Houk, and R. A. Shenvi, *Nat. Chem.*, 2020, **12**, 310.
26. F. Lovering, J. Bikker, and C. Humblet, *J. Med. Chem*., 2009, **52**, 6752.
27. M. D. Hanwell, D. E Curtis, D. C. Lonie, T. Vandermeersch, E. Zurek, and G. R. Hutchison, *J. Cheminf.*, 2012, **4**, 17.
28. Gaussian 16, Revision C.01, M. J. Frisch, G. W. Trucks, H. B. Schlegel, G. E. Scuseria, M. A. Robb, J. R. Cheeseman, G. Scalmani, V. Barone, G. A. Petersson, H. Nakatsuji, X. Li, M. Caricato, A. V. Marenich, J. Bloino, B. G. Janesko, R. Gomperts, B. Mennucci, H. P. Hratchian, J. V. Ortiz, A. F. Izmaylov, J. L. Sonnenberg, D. Williams-Young, F. Ding, F. Lipparini, F. Egidi, J. Goings, B. Peng, A. Petrone, T. Henderson, D. Ranasinghe, V. G. Zakrzewski, J. Gao, N. Rega, G. Zheng, W. Liang, M. Hada, M. Ehara, K. Toyota, R. Fukuda, J. Hasegawa, M. Ishida, T. Nakajima, Y. Honda, O. Kitao,

H. Nakai, T. Vreven, K. Throssell, J. A. Montgomery, Jr., J. E. Peralta, F. Ogliaro, M. J. Bearpark, J. J. Heyd, E. N. Brothers, K. N. Kudin, V. N. Staroverov, T. A. Keith, R. Kobayashi, J. Normand, K. Raghavachari, A. P. Rendell, J. C. Burant, S. S. Iyengar, J. Tomasi, M. Cossi, J. M. Millam, M. Klene, C. Adamo, R. Cammi, J. W. Ochterski, R. L. Martin, K. Morokuma, O. Farkas, J. B. Foresman, and D. J. Fox, Gaussian, Inc., Wallingford CT, 2016.